Chemical Physics 365 (2009) 24–29

Contents lists available at ScienceDirect

Chemical Physics

journal homepage: www.elsevier.com/locate/chemphys

THz oscillating currents enhanced by long-range correlations in DNA

Elena Díaz *, F. Domínguez-Adame

GISC, Departamento de Física de Materiales, Universidad Complutense, E-28040 Madrid, Spain

ARTICLE INFO

Article history:
Received 30 June 2009
Accepted 10 September 2009
Available online 16 September 2009

Keywords:
Charge transport in DNA
Large polaron
Disorder

ABSTRACT

Recently synthetic homopolymer DNA molecules have been theoretically demonstrated to support oscillating polarons when they are subjected to an external electric field (Bloch oscillations). Environment effects might introduce randomness in the molecular levels that, in general, destroy the coherence necessary to support this periodic dynamics. In this sense the existence of long-ranged correlations in DNA as well as its influence on its properties has been widely discussed. We demonstrate that the polaron performs Bloch oscillations even in disordered DNA molecules provided long-range correlations arise in the sequence of molecular levels. We predict the occurrence of THz alternating currents across the DNA molecules, opening the possibility of new applications in molecular electronics.

1. Introduction

Conducting properties of single DNA molecules have been studied for some years now due to their potential applications. Recent experiments suggest that DNA molecules may play an important role in future nanoelectronics. Thus, depending on the particular DNA sequence, environment conditions or contacts effects, different conducting behaviors have been established for the DNA [1]. The most promising DNA molecules seem to be DNA homopolymers as poly(G)–poly(C), whose semiconducting behavior has been theoretically and experimentally established [2–18].

However, since DNA is easily deformable, its structural deformations should be taken into account for an accurate description of its charge transport properties [19]. Charge coupling with such DNA distortions can create a polaron and enhance its mobility. This process reminds the multiple-step hopping mechanism also proposed to explain charge transport in DNA [20–22]. Thus, the behavior of the incoherent charge hopping can be understood as polaron diffusion. In this respect a variety of works have been devoted to the description of the polaron dynamics in DNA molecules [23–28].

For the particular case of DNA homopolymers subjected to a dc electric field, it was theoretically proven that, due to the periodicity of the nucleotide sequence, polarons might behave as electrons in biased periodic potentials. This means that they perform a periodic motion, in real and in k space, known as Bloch oscillations (BOs), whose amplitude and frequency can be established from semiclassical arguments [29,30]. Moreover, such a periodic motion leads to alternating currents in the THz range [31].

As we already mentioned, the particular nucleotide sequence as well as the environment conditions of DNA, which locally modify the base energy levels, strongly affect the transport properties. In this sense, it is well established the existence of long-range correlations in the energy landscape of natural DNA sequences [32–38] and therefore, a study of the polaron dynamics in such DNA molecules is in order. In particular, the energy distribution used in Ref. [39], which models long-range correlations, presents a number of interesting properties as reported in several works [39–44]. Despite disorder-induced dephasing effects, such correlated distributions support BOs when correlations are strong enough [42].

In this paper we study the polaron dynamics in DNA presenting long-range correlations. Contrary to what expected, long-range correlations in DNA enhance the periodic motion of the polaron under an applied electric field, leading to ac currents with a well-defined frequency in the THz range.

2. Model

The Peyrard–Bishop–Holstein (PBH) model maps the double stranded DNA helix onto a 1D lattice where every node represents a base pair [45]. A single degree of freedom is assigned to every site, which describes the stretching of the H-bonds within the two complementary bases, y_n. Notice that the stretch of the base pairs is the degree of freedom most strongly coupled to the electron system and therefore, the most capable of carrying polarons [46,47]. Moreover, due to the different time-scales of the carrier and the bases dynamics, the Hamiltonian of the PBH model can be cast within a semiclassical approximation [48]. The carrier is then treated quantum-mechanically, within the framework of the tight-binding approximation, while the lattice dynamics is taken into account classically. Under such considerations the Schrödinger

* Corresponding author. Tel.: +34 913944386; fax: +34 913944547.
E-mail address: elenadg@fis.ucm.es (E. Díaz).

0301-0104/$ - see front matter © 2009 Elsevier B.V. All rights reserved.
doi:10.1016/j.chemphys.2009.09.014

equation for the carrier in a biased heterogenous molecule is given by [49]

$$i\hbar\frac{d\psi_n}{dt} = \mathscr{E}_n - Un\psi_n - T(\psi_{n+1} + \psi_{n-1}) + \chi y_n\psi_n, \tag{1}$$

where ψ_n is the probability amplitude for the charge carrier located at the nth nucleotide ($n = 1,\ldots,N$). The parameter $U = eFa$ is the potential energy drop across one period of the lattice ($a = 3.4$ Å in DNA) due to the applied electric field F. The hopping is restricted to nearest-neighbor nucleotides and its magnitude is given by $-T$. The last term in Eq. (1) is a Holstein-like on-site correction to describe the carrier–vibration coupling, whose strength is parameterized by χ [50]. It should be noted that *ab initio* estimations of the coupling constant χ are scarce and the results are strongly dependent on the sequence and number of nucleotides [28]. In this work our calculations were mostly performed with the constant $\chi = 0.3$ eV/Å which agrees with the experimental and theoretical results given in Refs. [47,51].

Long-range correlations are introduced in the on-site energies $\mathscr{E}_n = \bar{\mathscr{E}} + \varepsilon_n$ as follows [39]

$$\varepsilon_n = \sigma C_\alpha \sum_{k=1}^{N/2} \frac{1}{k^{\alpha/2}} \cos\left(\frac{2\pi kn}{N} + \phi_k\right), \tag{2}$$

where $C_\alpha = \sqrt{2}\left(\sum_{k=1}^{N/2} k^{-\alpha}\right)^{-1/2}$ is a normalization constant and $\phi_1,\ldots,\phi_{N/2}$ are $N/2$ independent random phases, N assumed to be even. They are generated using a uniform probability distribution within the interval $[0, 2\pi]$. Hereafter we set $\bar{\mathscr{E}} = 0$ without loss of generality and the standard deviation of the sequence (2), $\sigma = \langle\varepsilon_n^2\rangle^{1/2}$, is referred to as magnitude of disorder. Here $\langle\ldots\rangle$ denotes average over realizations of the random phases ϕ_n. The strength of the correlations in the energy sequence is defined by the exponent α which also describes its power-like spectral density $S(k) \sim 1/k^\alpha$ [39]. When the electron–vibration coupling is neglected ($\chi = 0$), the steady-state Schrödinger equation arising from (1) supports a set of extended states at the band center as well as other interesting properties, provided $\alpha > \alpha_c \approx 2$ [39–43]. Therefore, we consider two limiting cases in our study hereafter, the strongly correlated case $\alpha > \alpha_c$ and the weakly correlated one $\alpha < \alpha_c$.

Newton's equations of motion for the displacement y_n become

$$m\frac{d^2y_n}{dt^2} = -V_M'(y_n) - W'(y_n, y_{n-1}) - W'(y_n, y_{n+1}) - \chi|\psi_n|^2, \tag{3}$$

where m is the nucleotide mass and the prime indicates differentiation with respect to y_n. The Morse potential

$$V_M(y_n) = V_0[\exp(-\alpha y_n) - 1]^2 \tag{4}$$

takes into account the anharmonic interaction between complementary bases as well as the interaction with the sugar–phosphate backbone and the surrounding solvent. The interaction between nearest-neighbor nucleotides along the stacking direction is described by the potential [49]

$$W(y_n, y_{n-1}) = \frac{k}{4}(2 + e^{-\beta(y_n + y_{n-1})})(y_n - y_{n-1})^2. \tag{5}$$

Both potential terms depend on fitting parameters which were chosen to reproduce experimental DNA melting curves [52]. Hereafter we will use the following set of optimized parameters: $m =$ 300 amu, $V_0 = 0.04$ eV, $\alpha = 4.45$ Å^{-1}, $k = 0.04$ eV/Å^2, $\beta = 0.35$ Å^{-1} and $T = 0.1$ eV. The chosen value of the parameter V_0 is compatible with poly(A)–poly(T) synthetic DNA [53].

3. Stationary polaron solution

To obtain the initial polaron, we closely follow the procedure given in Ref. [50] in an unbiased homogeneous lattice ($U = 0$ and $\sigma = 0$), including a dissipative term of the form $-\gamma m dy_n/dt$ in Eq. (3), with $\gamma = 50$ THz. We solve the nonlinear Eqs. (1) and (3) using a Runge–Kutta method of 4th order under rigid boundary conditions, considering the homopolymer DNA case. Gaussian functions are used as the initial conditions for the lattice distortion and the carrier wave function. Due to the dissipation in the lattice, the extra energy of these unphysical initial functions will be removed in the energy minimization process. After a long enough time we get the minimal energy conformation of the charge-lattice system, which is the stationary polaron solution to start our dynamical study of the biased DNA molecules.

In Fig. 1, the stationary polarons for different values of χ in a system of $N = 750$ are shown. It is to be noticed that by increasing the strength of the charge-lattice coupling the localization of the steady states becomes larger.

4. Motion of the polaron in a biased and disordered DNA molecule

In this section we calculate the time-evolution of the polaron obtained in Section 3. We integrate (1) and (3) including disorder in the site energies of a biased lattice without dissipation. The numerical integration method as well as the boundary conditions used in this case are the same that those considered above. Our interest is to monitor the polaron motion in a biased and disordered DNA molecule in the two already mentioned limiting cases: strongly correlated (i.e. $\alpha = 5$) and weakly correlated (i.e. $\alpha = 1$) disorder. To this end, the modulus of the carrier wave function $|\psi_n|$ and the local lattice distortion y_n will be displayed by means of density plots.

Figs. 2 and 3 show the local lattice displacement (left panels) and the corresponding modulus of the carrier wave function (right

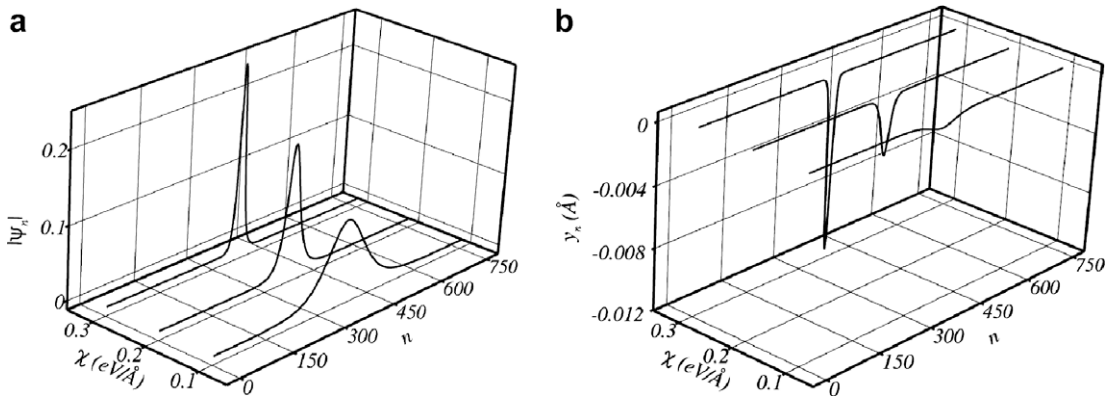

Fig. 1. (a) Modulus of the carrier wave function and (b) lattice displacement at $t = 0$ for different values of χ and $N = 750$.

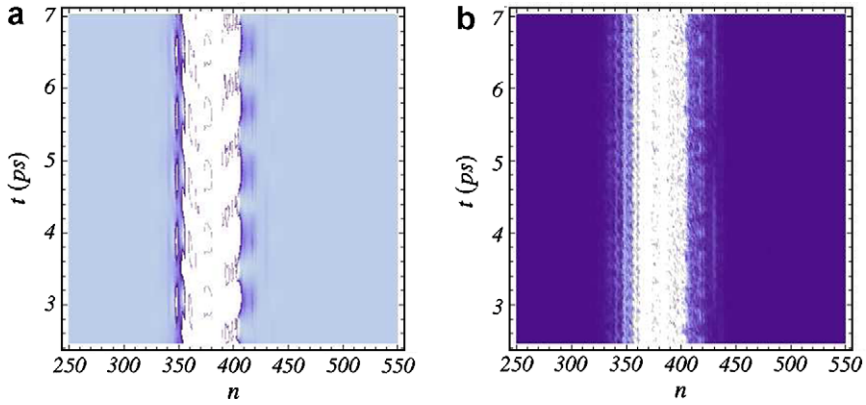

Fig. 2. (a) Local lattice displacement and (b) modulus of the carrier wave function in a lattice of $N = 750$ sites as a function of position and time for a single realization of disorder. The parameters considered are $\chi = 0.3$ eV/Å, $F = 3.0$ mV/Å, magnitude of disorder $\sigma = 0.1$ eV and correlation exponent $\alpha = 1$. Light and dark regions indicate nonzero and zero values, respectively.

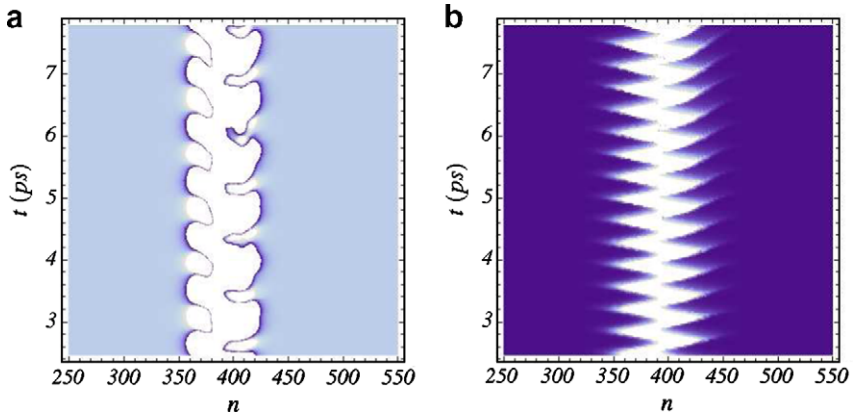

Fig. 3. Same as in Fig. 2 but considering the correlation exponent $\alpha = 5$.

panels) in a lattice of $N = 750$ sites as a function of position and time for a single realization of disorder. The parameters considered are $\chi = 0.3$ eV/Å, $F = 3.0$ mV/Å, and magnitude of disorder $\sigma = 0.1$ eV. Notice that this magnitude of disorder is of the order of the nearest-neighbor hopping T. The correlation exponent is $\alpha = 1$ in Fig. 2 (weak correlations) while $\alpha = 5$ in Fig. 3 (strong correlations).

No signatures of BOs are revealed in the wave packet dynamics shown in Fig. 2b, as a clear indication of the occurrence of disorder-induced dephasing effects, expected in the weakly correlated regime [42]. However, the lattice dynamics seems to present weak traces of a periodic time-evolution, as seen in Fig. 2a. On the contrary, at $\alpha = 5$ in Fig. 3, the density plots show well behaving oscillations of the carrier and the lattice, demonstrating that strong correlations enhance the coherence necessary for sustained BOs to arise.

In order to make clear which frequencies are involved in the carrier and the lattice time-evolution, we calculate the Fourier spectrum of the time-dependent magnitudes $c(t)$ and $l(t)$, defined as follows

$$c(t) = x(t) - x(0), \quad x(t) = \sum_{n=1}^{N} n|\psi_n(t)|^2, \tag{6a}$$

$$l(t) = \xi(t) - \xi(0), \quad \xi(t) = \sum_{n=1}^{N} n y_n(t)/a. \tag{6b}$$

The lower panel of Fig. 4a confirms that in the case of weakly correlated systems, no well defined oscillations are performed by the wave packet of the carrier and therefore, a variety of several peaks arise in the Fourier spectrum of its centroid, $c(t)$. On the contrary, in the upper panel the analogous magnitude for the lattice distortion, $l(t)$, reveals a clear oscillatory behavior, as we already presumed in the preceding paragraph. Similarly to what happens in the case of the homogeneous molecule (see Ref. [31]), it oscillates with a main frequency of 7.22 THz close to the Morse frequency of the system $\omega_M = \alpha\sqrt{2V_0/m} = 7.138$ THz according to its Fourier spectrum. Nevertheless, in the disordered situation there is no other peak related to the Bloch frequency which indeed appeared in the homogeneous molecule [31]. Therefore, we claim that the dynamics of the disordered molecule is mainly defined by the Morse potential and it is even more decoupled from the carrier one than in homogeneous DNA molecules.

On the other hand, Fig. 4b confirms the results observed in Fig. 3 for the strongly correlated regime. Thus, well behaving BOs appear in the time-evolution of the magnitudes $c(t)$ and $l(t)$. The Fourier spectrum of $l(t)$ turns out to be single-peaked again at the Morse frequency as in the weakly correlated regime, while that associated to $c(t)$ reveals now a well defined peak at 17.0 THz. Notice that this frequency is shifted with respect to the semiclassical expected value of the Bloch frequency $\omega_B = eFa/\hbar = 15.502$ THz.

This deviation can be understood by looking at the particular energy landscape of the considered realization of disorder. To this

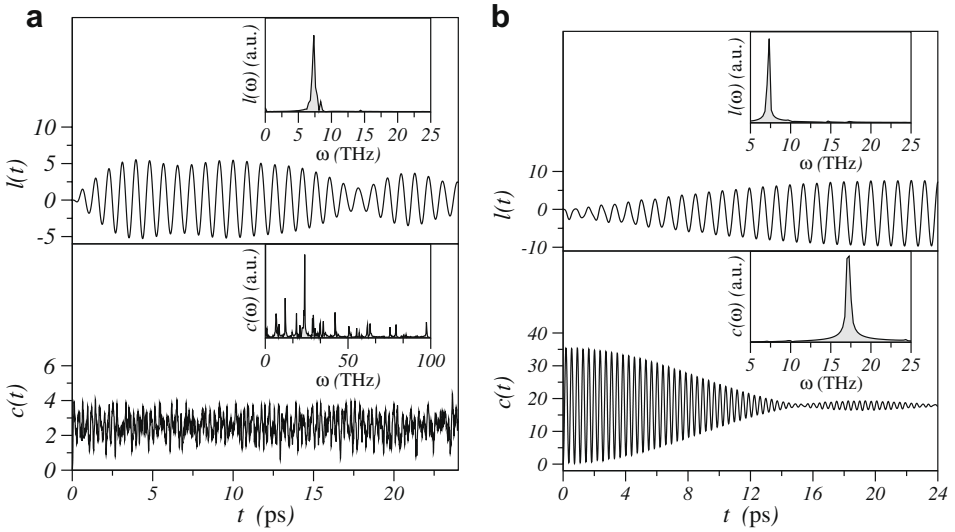

Fig. 4. Centroid of the carrier wave function, $c(t)$, and $l(t)$ as a function of time in a disordered lattice of $N = 750$ sites for $\chi = 0.3$ eV/Å and $F = 3.0$ mV/Å. The magnitude of disorder is set to $\sigma = 0.1$ eV and the correlation exponents are (a) $\alpha = 1$ and (b) $\alpha = 5$. The insets show the corresponding Fourier transforms.

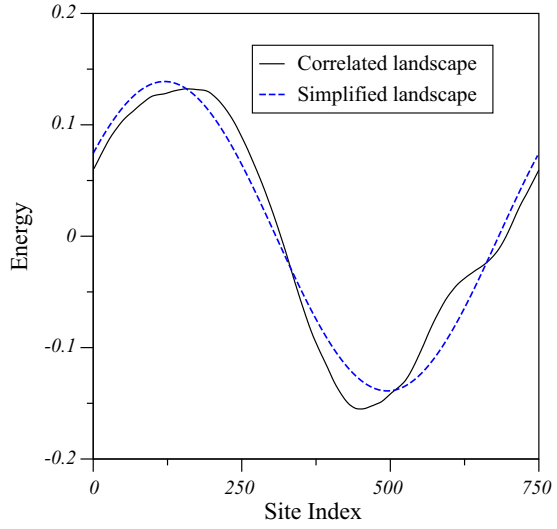

Fig. 5. Energy landscape for a single realization of the disorder distribution Eq. (2) for a correlation exponent $\alpha = 5$ and a system of $N = 750$ sites. The simplified energy landscape defined by the first term of the distribution is also displayed.

end, we take advantage of the simplification proposed in Ref. [43] for strong correlated systems (see Fig. 5). According to that approach, in the case of strong correlations the whole distribution (2) can be substituted by the first term of the sum

$$\varepsilon_n \approx \sigma C_\alpha \cos(2\pi n/N + \phi_1). \tag{7}$$

This is the dominant term in (2) when α is large, which is given by the random phase ϕ_1. In our simulation the phase randomly generated was $\phi_1 = 5.28$ rad. Fig. 5 shows the actual energy landscape of the single realization used in our simulations as well as the simplified one (7). Notice that such an energy landscape gives rise to a new tilted potential at the center of the lattice, which is to be added to the linear applied bias.

The effective potential drop across one lattice period created by (7) at the initial mean position of the polaron $N/2$ is $U_{\text{eff}} = \xi_\alpha \sin\phi_1$, with $\xi_\alpha = 2\pi\sigma C_\alpha/Na$. In the case of our random realization ($\phi_1 = 5.28$ rad) it results in an effective bias of $U_{\text{eff}} \approx -1.0$ meV/Å. The term $U_{\text{eff}} n$ is to be added to Eq. (1) in such a way that the potential energy drop across one period of the lattice becomes now $-(U - U_{\text{eff}})$. Thus, the semiclassical Bloch frequency under such conditions is $\omega_B^* = (U - U_{\text{eff}})/\hbar \approx 17.0$ THz, which is in prefect agreement with the position of the single peak revealed by the Fourier spectrum of the centroid $c(t)$ (see Fig. 4b). It is worth mentioning that the effective potential created by (2) was approximated by a linear profile at the center of the molecule. In those realizations of disorder where this is not the case, the previously introduced effective potential drop U_{eff} is actually not well defined. Thus, despite finding well behaving oscillations of the wave function, the Fourier spectrum of $c(t)$ becomes more complex, presenting several peaks around the semiclassical value of the Bloch frequency.

For completeness we also study the dynamics of the wave function for different values of the carrier-lattice coupling and applied bias in the strongly correlated limit. Bear in mind that the lattice dynamics is defined in all cases by the Morse potential, not depending on the remaining model parameters as we already demonstrated. Our results, summarized in Fig. 6, show that for all considered parameters the carrier wave function performs well behaving oscillations, whose amplitude and period depend on the bias strength as expected for BOs, namely $L_B \propto 1/U$ and $\tau_B \propto 1/U$ [29,30]. On the other hand, these oscillations behave similarly for different values of the carrier-lattice coupling. In this respect notice that for a small coupling (i.e. $\chi = 0.1$ eV/Å) the polaron extends over a larger number of nucleotides and it is more easily affected by disorder effects, leading to a faster transformation of the initial shape of the wave packet. We stress that the DNA molecule should be long enough to support the oscillating carrier dynamics at low fields (the amplitude of the BOs increases by decreasing the applied bias).

5. Average current density

In view of the oscillatory motion performed by the wave packet of the carrier in the strongly correlated regime, a similar time-dependent dynamics is expected for the average current density defined as follows [49]

$$J(t) = \frac{he}{m_e N a^2} \sum_{n=1}^{N} \text{Im}\left[\psi_n^*(\psi_{n+1} - \psi_{n-1})\right]. \tag{8}$$

Here m_e is the mass of the carrier. Indeed, the oscillation frequency of $J(t)$ is slightly shifted from the predicted Bloch frequency in

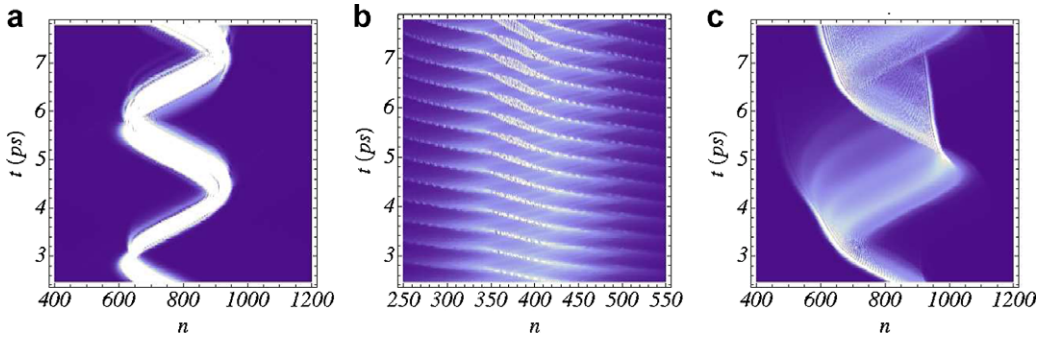

Fig. 6. Modulus of the carrier wave packet as a function of position and time for a single realization of disorder ($\sigma = 0.1$ eV and $\alpha = 5$). The considered parameters for the biased molecule are the following: (a) $N = 750, \chi = 0.3$ eV/Å and $F = 0.3$ mV/Å, (b) $N = 1250, \chi = 0.1$ eV/Å and $F = 3.0$ mV/Å and (c) $N = 1250, \chi = 0.1$ eV/Å and $F = 0.3$ mV/Å.

disordered lattices. Moreover, this shift was proven to depend on the particular realization of disorder in the previous section. Therefore, by considering the Fourier transform $J(\omega)$ of an ensemble of disordered sequences, one can obtain the frequency probability distribution of $J(t)$ centered at the semiclassical Bloch frequency. The width of this distribution, σ_ω, might be estimated within the same reasoning introduced in the preceding section: the effective disorder-induced bias U_{eff} is proportional to the frequency shift of the Fourier peak of $J(\omega)$ with respect to the semiclassical value ω_B. Thus, its probability distribution coincides with the one of the shifted frequencies of $J(t)$ for different realizations of disordered sequences.

This probability distribution can be analytically calculated keeping in mind that the randomness of (2) arises from the set of $N/2$ independent random phases $\phi_1, \ldots, \phi_{N/2}$ uniformly distributed within the interval $[0, 2\pi]$. Therefore, one can write $\mathscr{P}(U_{\text{eff}})\, dU_{\text{eff}} = \mathscr{P}(\phi)\, d\phi$ and the following distribution for the effective fields is obtained

$$\mathscr{P}(U_{\text{eff}}) = \frac{1}{\pi\sqrt{\xi_\alpha^2 - U_{\text{eff}}^2}}, \tag{9}$$

with $|U_{\text{eff}}| \leqslant \xi_\alpha$. This probability distribution diverges at the edges and its width is given by $\sigma_\omega = 2\xi_\alpha$. Thus, it is inversely proportional to the number of base pairs N.

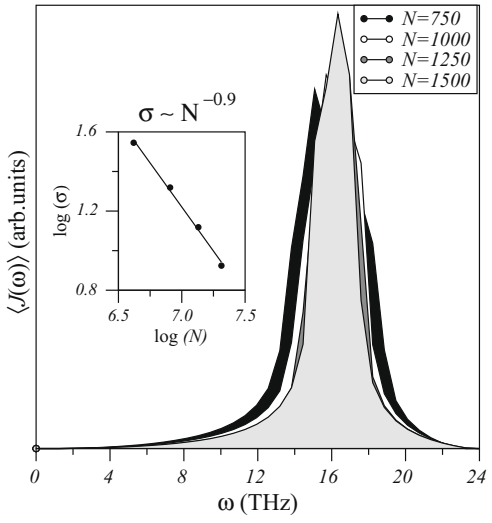

Fig. 7. Average Fourier transform of the current density $J(t)$ of 100 different realizations of disorder. The parameters used in the calculations are $\chi = 0.1$ eV/Å, $F = 3.0$ mV/Å, $\sigma = 0.1$ eV and $\alpha = 5$. Four different sizes of the system are considered. The inset displays $\log(\sigma_\omega)$ versus $\log(N)$ as well as the fitting of the data.

Our numerical calculations prove the validity of the above approach. To this end, we calculate $J(t)$ and the average Fourier spectrum $\langle J(\omega)\rangle$ for an ensemble of disorder realizations. We repeat this procedure for four different sizes of the system $N = 750, N = 1000, N = 1250$, and $N = 1500$ and display simultaneously our results in Fig. 7. This figure clearly demonstrates that the width of $\langle J(\omega)\rangle$ decreases upon increasing the number of nucleotides. This means that disorder effects are less relevant in longer molecules and therefore, the average current density oscillates with a frequency closer to the Bloch frequency.

On the other hand, our calculations are in good agreement with the above proposed approach to describe the dispersion of the oscillation frequencies of $J(t)$ in disordered systems. We find a size-dependence $\sigma_\omega \propto 1/N^{0.90}$, close to that predicted $\sigma_\omega \propto 1/N$. Needless to say that the different exponent comes from the approximations considered in our approach, namely the replacement of the energy landscape by a sine-like function, the absence of the charge-lattice coupling and the definition of the U_{eff} as the effective bias created at a single site of the molecule.

6. Conclusions

The polaron dynamics was studied in synthetic DNA molecules with long-range correlations in the sequence of molecular levels. It is well established that, neglecting the charge-lattice interaction, the electron undergoes coherent and harmonic oscillations in biased uniform lattices, known as Bloch oscillations [29,30]. Besides, in a recent work [31] it was theoretically demonstrated that these oscillations might even occur when dealing with polaron states within the PBH model, which accurately describes the DNA dynamics [45,48–50,52]. This leads to the existence of oscillating currents across DNA homopolymers.

We have focused on sequences presenting long-range correlations [32–38]. Therefore, the molecular levels of the nucleotides were generated according to the long-range correlated sequence proposed in Ref. [39]. Regarding the long-range correlations effects, and despite the disorder-induced dephasing processes, we still found an oscillatory carrier dynamics for strong correlations. Its frequency turned out to be shifted with respect to the semiclassical value of the Bloch frequency. We theoretically explained this shift by extending a simplified approach formerly proposed in Ref. [43].

The oscillatory carrier dynamics leads to alternating currents across the DNA molecule whose frequency lies in the THz range, which might be useful in nanoelectronic applications. We calculated the averaged Fourier transform of the electric current in an ensemble of disordered DNA sequences. The frequency dispersion around the Bloch frequency decreases by considering larger systems, where disorder effects seem to be less relevant. We were

able to explain this conclusion by means of the simplified analytical approach.

It is to be mentioned that, apart from the disorder-induced effects, scattering by phonons also destroys the phase coherence at times larger than the scattering time τ and therefore, BOs can hardly be observed at such time-scales. Lakhno and Fialko [27] estimated that the temperature $T_{\min}$ below which BOs take place at a given magnitude of the electric field is $T_{\min} \simeq 0.45 T_0 (\omega_B \tau_0)^{1/2.3}$. For instance at the field magnitude $F = 3.0$ mV/Å, BOs might be observed at $T < T_{\min} = 50$ K. Larger electric fields are applied in the conducting experiments on DNA which raise this threshold temperature.

Acknowledgements

The author thanks R.P.A. Lima, R. Brito and E. Maciá for helpful discussions. This work was supported by MEC (Project MOSAICO) and BSCH-UCM (Project PR34/07-15916).

References

[1] D. Porath, G. Cuniverti, R. Di Felice, Top. Curr. Chem. 237 (2004) 183.
[2] D. Porath, A. Bezryadin, S. de Vries, C. Dekker, Nature 403 (2000) 635.
[3] K.-H. Yoo, D.H. Ha, J.-O. Lee, J.W. Park, J. Kim, J.J. Kim, H.-Y. Lee, T. Kawai, H.Y. Choi, Phys. Rev. Lett. 87 (2001) 198102.
[4] B.Q. Xu, P.M. Zhang, X.L. Li, N.J. Tao, Nano Lett. 4 (2004) 1105.
[5] H. Cohen, C. Nogues, R. Naaman, D. Porath, Proc. Natl. Acad. Sci. 102 (2005) 11589.
[6] S. Roy, H. Vedala, A. Datta Roy, D.-H. Kim, M. Doud, K. Mathee, H.-K. Shin, N. Shimamoto, V. Prasad, W. Choi, Nano Lett. 8 (2008) 26.
[7] K. Iguchi, Int. J. Mod. Phys. B 11 (1997) 2405.
[8] K. Iguchi, J. Phys. Soc. Jpn. 70 (2001) 593.
[9] G. Cuniberti, L. Craco, D. Porath, C. Dekker, Phys. Rev. B 65 (2002) 241314.
[10] S. Roche, D. Bicout, E. Maciá, E. Kats, Phys. Rev. Lett. 91 (2003) 228101.
[11] K. Iguchi, Int. J. Mod. Phys. 13 (2004) 1845.
[12] V.M. Apalkov, T. Chakraborty, Phys. Rev. B 71 (2005) 033102.
[13] H. Mehrez, M.P. Anantram, Phys. Rev. B 71 (2005) 115405.
[14] D. Klotsa, R.A. Römer, M.S. Turner, Biophys. J. 89 (2005) 2187.
[15] A. Rodríguez, R.A. Römer, M.S. Turner, Phys. Stat. Solidi B 243 (2006) 373.
[16] A.V. Malyshev, Phys. Rev. Lett. 98 (2007) 096801.
[17] E. Maciá, S. Roche, Nanotechnology 17 (2006) 3002.
[18] E. Díaz, A.V. Malyshev, F. Domínguez-Adame, Phys. Rev. B 76 (2007) 205117.
[19] E.M. Conwell, S.V. Rakhmanova, Proc. Natl. Acad. Sci. USA 97 (2000) 4556.
[20] D. Ly, Y. Kan, B. Armitage, G.B. Schuster, J. Am. Chem. Soc. 118 (1996) 8747.
[21] J. Jortner, M. Bixon, T. Langenbacher, M.E. Michel-Beyerle, Proc. Natl. Acad. Sci. USA 95 (1998) 12759.
[22] Y.A. Berlin, A.L. Burin, M.A. Ratner, J. Phys. Chem. A 104 (2000) 443.
[23] C-M. Chang, A.H. Castro, A.R. Bishop, Chem. Phys. 303 (2004) 189.
[24] H. Yamada, E.B. Starikov, D. Hennig, Eur. Phys. J. B 59 (2007) 185.
[25] E. Maciá, Phys. Rev. B 76 (2007) 245123.
[26] S.V. Rakhmanova, E.M. Conwell, J. Phys. Chem. B 105 (2001) 2056.
[27] V.D. Lakhno, N.S. Fialko, Pis'ma ZhETF 79 (2004) 575.
[28] J.A. Berashevich, V. Apalkov, T. Chakraborty, J. Phys.: Condens. Matter 20 (2008) 075104.
[29] F. Bloch, Z. Phys. 52 (1929) 555.
[30] C. Zener, Proc. Roy. Soc. London, Ser. A 145 (1934) 523.
[31] E. Díaz, R.P.A. Lima, F. Domínguez, Phys. Rev. B 78 (2008) 134303.
[32] P. Carpena, P. Bernaola-Galván, P. Ch. Ivanov, H.E. Stanley, Nature 418 (2002) 955;
P. Carpena, P. Bernaola-Galván, P. Ch. Ivanov, H.E. Stanley, Nature 421 (2003) 764.
[33] S. Roche, Phys. Rev. Lett. 91 (2003) 108101.
[34] S. Roche, D. Bicout, E. Maciá, E. Kats, Phys. Rev. Lett. 91 (2003) 228101.
[35] M. Unge, S. Stafstrom, Nano Lett. 3 (2003) 1417.
[36] P. Carpena, P. Bernaola-Galán, Ch. Ivanov, Phys. Rev. Lett. 93 (2004) 176804.
[37] S. Roche, E. Maciá, Mod. Phys. Lett. 18 (2004) 847.
[38] H. Yamada, Phys. Lett. A 332 (2004) 65.
[39] F.A.B.F. de Moura, M.L. Lyra, Phys. Rev. Lett. 81 (1998) 3735.
[40] F.M. Izrailev, A.A. Krohin, Phys. Rev. Lett. 82 (1999) 4062.
[41] H. Shima, T. Nomura, T. Nakayama, Phys. Rev. B 70 (2004) 075116.
[42] F. Domínguez-Adame, V.A. Malyshev, F.A.B.F. de Moura, M.L. Lyra, Phys. Rev. Lett. 91 (2003) 197402.
[43] E. Díaz, A. Rodríguez, F. Domínguez-Adame, V.A. Malyshev, Europhys. Lett. 72 (2005) 1018.
[44] E. Díaz, F. Domínguez-Adame, Y. Kosevich, V.A. Malyshev, Phys. Rev. B 73 (2006) 174210.
[45] M. Peyrard, A.R. Bishop, Phys. Rev. Lett. 62 (1989) 2755.
[46] S.S. Alexandre, E. Artacho, J.M. Soler, H. Chacham, Phys. Rev. Lett. 91 (2003) 108105.
[47] E.B. Starikov, Phil. Mag. 85 (2005) 3435.
[48] G. Kalosakas, S. Aubry, G.P. Tsinronis, Phys. Rev. B 58 (1998) 3094.
[49] P. Maniadis, G. Kalosakas, K.O. Rasmussen, A.R. Bishop, Phys. Rev. E 72 (2005) 021912.
[50] S. Komineas, G. Kalosakas, A.R. Bishop, Phys. Rev. E 65 (2002) 061905.
[51] A. Omerzu et al., Phys. Rev. Lett. 93 (2004) 218101.
[52] T. Dauxois, M. Peyrard, Phys. Rev. E 47 (1993) R44.
[53] J.X. Zhu, K.O. Rasmussen, A.V. Balatsky, A.R. Bishop, J. Phys.: Condens. Matter 19 (2007) 136203.